PRL-TN-2014-107
Technical Note

An automated CCD-based Multi-wavelength Airglow Photometer (CMAP) for Optical Aeronomy studies

by

K. A. Phadke, R. Narayanan, R. P. Singh and D. Pallamraju

भौतिक अनुसंधान प्रयोगशाला, अहमदाबाद
Physical Research Laboratory, Ahmedabad

Published by
The Dean's office, PRL.

An Automated CCD-based Multi-wavelength Airglow Photometer (CMAP) for Optical Aeronomy Studies

Kedar A. Phadke*[1], R. Narayanan[1], Ravindra P. Singh[1] and Duggirala Pallamraju[1]

Abstract
The technical details on the development of a **C**CD (charge coupled device) based **M**ulti-wavelength **A**irglow **P**hotometer (CMAP) and its in-house built software are described in this report. This combination of hardware and software makes CMAP capable of operating in an automated and unattended mode, even in a remote location. CMAP uses CCD as the detector which makes the system low cost, reliable, and rugged for field operations. To enable CMAP operations nearly simultaneously at multiple wavelengths, a temperature stabilized filter wheel was developed which can accommodate five different filters at a time. We have used narrow-band interference filters, the transmission of which is prone to temperature fluctuations. In order to restrict the temperature fluctuations to as low as $\pm 0.1^{\circ}$C we have mounted Peltier elements on the filter wheel and then encased the assembly in a Teflon box. We have also developed temperature monitoring electronics and a MFC (Microsoft Foundation Class) based application which can control the CCD and filter wheel operations in a pre-defined mode, which can be programmed to provide the data files in FITS format. The components for development of CMAP were selected making sure that they were compatible with each other and could be operated using a single software. All of these features make CMAP quite capable in enabling operations in an unattended mode when commissioned in a field station. The ability of CMAP to provide nightglow emission intensities at multiple wavelengths almost simultaneously enables investigations of various aspects of the upper atmospheric dynamics and coupling processes.

[1] *Space & Atmospheric Sciences Division, Physical Research Laboratory, Ahmedabad*
***Corresponding author**: kedar@prl.res.in

Contents

1. Background

The Earth's upper atmosphere is highly variable in nature. Several photochemical, chemical, and dynamical processes take place in this region. Depending on energy state of the atmospheric species, different photochemical and chemical reactions occur in response to the incident solar radiation. As a result, various neutrals, ionized atoms and molecules get to their excited states. During their de-excitation, photons are emitted that are characteristic of the energy state of emitting species which range from ultraviolet to infrared wavelengths of the electromagnetic spectrum and this is called airglow. This optical phenomenon causes the night sky to never be completely dark (even after the effects of starlight and diffused sunlight from the far side of the sky are removed) and could contribute to as much as 50% of the total luminosity of the night sky [Priedhorsky, 1996].

Airglow measurements form a good tracer to investigate the neutral behaviour of the upper atmosphere which can be measured using different optical techniques; namely photometry, interferometry, and spectrometry. In this report we will discuss about the development of a photometer (which measures the volume integrated airglow emission intensities) and a software for its automated operation. In PRL, use of photometry had begun with the setting up of Mt. Abu Observatory since 1960s [Pallamraju D., CAWSES-II, TG4 Newsletter Vol. 8, April, 2012] when OI 630 nm emissions were observed using a large bandwidth filter. Such photometers were used the world over using photo-multiplier tube (PMT) as the detector. With the advent of large format CCDs, the emphasis changed from photometry to imaging of optical airglow emissions. At PRL, the use of nightglow photometry was revived when concomitant finer features of OI 630 nm nightglow emissions were obtained when their field of view (FOV) was kept equal to that of the VHF radar (of $\sim 3^{\circ}$) [e.g., Chakrabarty D, 2007, Sekar et al., 2012]. In the recent past, there is a growing realization globally on the adverse effects/consequences of several large scale geophysical phenomenon such as, space

weather and sudden stratospheric warming (SSW) in the near Earth space. Further, there is a growing importance on the investigations on vertical coupling process of atmospheric regions [Pallamraju D., et al., 2012] wherein it is essential to investigate the behavior of atmosphere almost continuously. It can be achieved by passively remote sensing the upper atmosphere by measuring airglow emission intensities at multiple wavelengths simultaneously. In order to achieve it, it is imperative that measurement techniques operate continuously and reliably in an unattended manner. Due to the advent of solid state based CCD-chips, which are rugged, inexpensive, and programmable, these have been made use of as the detector as opposed to the conventional PMT in CMAP. This report elucidates the development of a new multiple wavelength photometer along with the software developed in-house for automation of the system which enables measurement of night time airglow emission intensities with a high signal to noise ratio (SNR) and data cadence.

2. Photometers

2.1 Conventional photometers

Conventionally, airglow photometric studies are carried out using photo-multiplier tube (PMT) as the detector. Although, PMT-based photometers are being used since long, operations of PMT requires high voltage (typically $\sim$ 1.5 kV), pre-amplifier discriminator, and photon counter devices. Efforts have been made to run such photometers in an automated mode. However, the use of high voltage devices in PMT-based systems prevents reliable unattended operations. Further, overexposure of a PMT damages the photocathode. The quantum efficiency (QE) of the PMT depends on the substrate used. For example, a GaAsP photocathode has a QE greater than 30% for the wavelength range 450 - 600 nm with a peak QE of 40%, whereas, for a GaAs photocathode the quantum efficiency is just greater than 10% for 500 - 850 nm range with a peak of 12% (e.g., Hamamatsu, H-7421). For optical aeronomy studies, important emissions exist in the wavelength range of 400-900 nm; thus, two different PMTs are required to be used depending on their spectral coverage (one for wavelength range 450-600 nm and the other for 500-850 nm) in order to not compromise on the QE. Simultaneous operation with two PMT is not possible, thereby requiring two independent optical systems for measuring emissions in the whole visible spectral range.

2.2 CMAP

With the advent of CCDs during last couple of decades, its applications are growing in different imaging techniques used in different branches of science. Although CCDs are widely used in imaging techniques, the availability of small-format (size of pixels), and low-cost CCDs in the recent past, offer a viable alternative to the conventional PMTs in airglow photometers. CCDs have semi-conductor chips as detectors and are generally insensitive to over-exposure as compared to PMTs. PMTs have photocathode as a detector in which the current generated is directly proportional to the level of incident light. If the PMT is overexposed, the higher currents generated can even damage the anode and can make it light insensitive either temporarily or permanently. Whereas, in CCDs the light level is stored by charging capacitors and thus are not damaged even if over-exposed. Therefore, CCDs offer more durable, reliable, and hassle-free operation in comparison to PMTs. Moreover, CCDs provide broader spectral coverage as compared to PMT with high QE, therefore, airglow emissions that are widely separated in wavelength can be accommodated by using a single CCD. Further, as no high-voltage is involved with the functioning of CCDs, it is possible to commission them in field stations in an unattended mode for risk-free operations. It is relevant to note that the cost of the type of CCD being discussed here is a factor of six less than the PMTs that are generally used for such measurements. Due to this, use of CCD as the detector also reduces the cost of the instrument. The one flip side of CCDs in comparison to PMTs is that the signal contains read-out noise which needs to be considered in the SNR calculation which reduces data cadence. However, as it will be discussed in section 5, the SNR of our measurements is around 100. Thus, this read out noise does not adversely affect CMAP data quality. Also the data cadence is much better ($\sim$1 minute) than the natural period of oscillations (Brunt Vaisala) of emissions emanating from the lowest altitude where the Brunt Vaisala period is the smallest ($\sim$5 minutes). For the development of CMAP we have chosen a commercially available CCD Atik 314L+ which uses Sony ICX285AL ExView 1392 x 1040 sensor, having a pixel size of 6.45μm with the total size of the chip being 8.98 x 6.71 mm. The QE of this detector is above 40% for wavelengths from 420 nm to 770 nm[5]. Some of the salient features of this CCD are summarized below:

- USB2 performance for ultra-fast download speeds
- 1 megapixel/second readout
- Lightweight (approx. 400 g), low power consumption: 12V, 0.8A
- Thermoelectric cooling: 27° C below ambient temperature
- Software-controlled cooling for automated operation.

As stated earlier, the CCD is an array detector; since we are interested in photometry, the CCD can be used in super-pixel mode, wherein 32 pixels are binned in both x and y directions in order to increase the SNR as the readout noise is reduced due to on-chip binning [Pallamraju D., 2003]. From the images obtained by the photometer, the total counts in the illuminated region are calculated after subtracting the dark noise which yields intensity of the airglow emissions.

3. Elements of CMAP

The development of a fully automated CCD-based Multi-wavelength Airglow Photometer (CMAP) is discussed in this

section. It is required that there is perfect synergy between the in-house developed software and all the hardware components of CMAP for its smooth functioning. For this, all the hardware parameters, namely, the filter temperature, movement of filters, azimuth and elevation angles of mirror scanner, the CCD temperature, on-chip binning, exposure times, data storage location, and format, etc. are monitored and controlled by the software (development of software discussed in section 3.2). On the hardware side, fabrication of temperature controlled filter wheel chamber and microprocessor controlled mirror scanner was required along with the whole assembly for CMAP. All these components were developed, assembled and tested in PRL and interfaced with the software developed in-house.

3.1 Hardware components of CMAP

This section gives an overview of all the components that are integrated in CMAP. The optical configuration as shown in Figure 1 consists of field lens, aperture, collimating lens, filter assembly, imaging lens, and detector. The CCD used in CMAP has been already discussed in section 2.2. The filter wheel assembly has provision to house five filters. This filter wheel assembly has to be temperature controlled for proper functioning of the filters. Thus, a temperature monitoring and control system was developed for the filter wheel assembly. The light from each filter; brought into the optical path in predefined sequence is focussed onto the CCD-detector using an imaging lens. In the following sub-sections the components listed above will be described along with their importance in CMAP.

3.1.1 Schematic of CMAP

As can be seen in Figure 1, CMAP consists of fore optics, filter and imaging sections. The main objective of the front-end optics is to collimate the light and make this parallel beam of light to fall normally on the interference filters. The filtered light is then made to fall on the imaging lens which focuses the photons from the interference filter onto the CCD chip. F/2 optical configuration is used for the photometer (Refer Figure 1). The combination of the field lens and the aperture decides the FOV of the system. The FOV of the system is given by $(\tan^{-1}(\frac{d}{f}))$, where d is the diameter of the aperture and f is the focal length of the objective lens. Since, we are using a CCD detector, the chip size and the focal length of the imaging lens will decide the maximum FOV that can be imaged onto the detector. In order to enable comparison with a PMT based system (FOV $\sim 3^{\circ}$), we have used 9 mm aperture size with 100 mm focal length objective lens i.e. FOV of $\sim 5^{\circ}$, but appropriate region on the CCD chip was selected (2.5 mm diameter circle) for integrating the counts to compare with PMT based system. Since the chip size of the CCD being used is 8.98 x 6.71 mm, a shorter focal length of 50 mm imaging lens is used so that the photons from the whole aperture can be imaged onto the chip. The central area of the chip illuminated will be of diameter 4.5 mm. With this design, the aperture size can be increased even up to 11 mm without any loss of photons. The counts obtained from the pixels illuminated with photons from airglow are integrated during analysis and after subtracting the dark noise, information on the nightglow emission intensities is obtained.

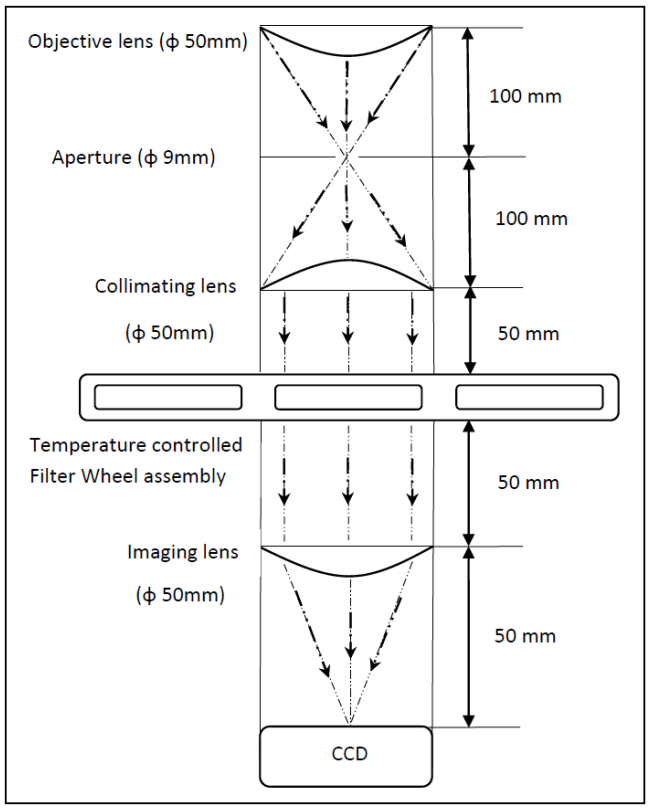

Figure 1. The Optical configuration of CMAP (not to scale).

3.1.2 Filter Wheel Assembly

Conventional photometers usually involve the use of a single filter per system as the PMT quantum efficiency may not be suitable for monitoring emissions at multiple wavelengths. As in the case of CCDs this limitation is overcome, it makes way for the use of filters covering a broader range of wavelengths. The Filter Wheel used in our system is Atik EFW2 which accommodates five filters of two-inch diameter.

The filters used for the airglow measurements are narrow-band interference filters with 0.3 nm bandwidth transmission around the central wavelength at $\sim 23^{\circ}$C. Interference filters are multi-layer coated thin film devices. The principle of operation of an interference filter is analogous to a lower-order Fabry-Perot etalon [Thorne, Spectrophysics, 1999]. The spectral (wavelength) rejection is done by creating destructive interference conditions, whereas, constructive interference occurs for the wavelength of interest. A narrow band interference filter generally consists of several elements called cavities, separated by absentee layer (low refractive index material). Multi-cavity design drastically reduces the transmission of light from out-of-band spectral region.

The wavelength of peak transmittance of such filters for small angles (ϕ) of incidence (up to $\sim 15^\circ$) is given by:

$$\lambda_t = \lambda_i \sqrt{1 - (\frac{n_o}{n_e})^2 \sin^2 \phi} \quad (1)$$

where n_o is the refractive index of the external medium (n_o=1 for air) and n_e is the "effective refractive index" of the spacer. λ_t and λ_i are the transmitted and incident wavelengths, respectively. As we are using a collimating lens, the incident light will fall normally onto the filters thereby not changing the wavelength of peak transmittance. In addition to the dependence on the angle of incidence, the wavelength of peak transmittance of an interference filter also depends on the temperature, as a change in temperature alters the refractive index of the medium. Thus, the wavelength of peak transmittance of the spectrum shifts slightly ($\sim$0.02 nm/K)[4] to longer/shorter wavelength with increasing/decreasing temperature and hence the temperature has to be maintained for these interference filters, otherwise it will allow light from the spectral regions other than that intended for use. For this purpose, a temperature controlled chamber using peltier elements has been built in-house to augment with the commercially available filter wheel. A temperature monitoring system was developed to augment with a commercially available control system for this filter wheel assembly which can maintain temperature to an accuracy of $\pm 0.1^\circ$ C.

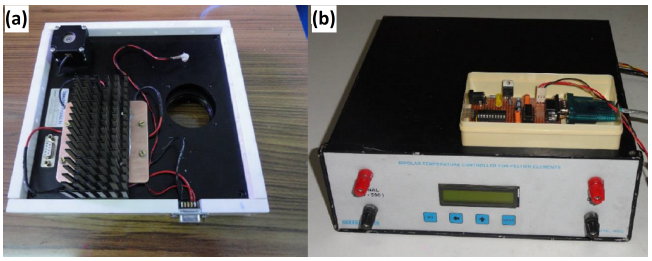

Figure 2. (a) The augmentation done to filter wheel enabling it to control the temperature. (b) Bipolar temperature controller which is commercially available is used to regulate the current supplied to the TEC units attached to filter wheel.

3.1.3 Filter Wheel temperature monitoring and control

The required software and hardware for the filter wheel monitoring system was developed in-house, in which for temperature monitoring AD590 temperature sensor was used. The output of this temperature sensor was given as an input to the custom made bipolar temperature controller. The temperature controller (Figure 2b) with this given input calculates the amount of current to be supplied to the peltier elements for them to control the temperature of the filter wheel assembly and its polarity. Four Thermoelectric cooler (TEC) units of dimensions 40 mm by 40 mm were attached to the filter wheel assembly (Figure 2a) and the assembly was insulated from ambient environment by using an additional insulating box made of Teflon (Figure 3). A software tool has been developed by which temperature values can be stored in a predefined format for temperature monitoring.

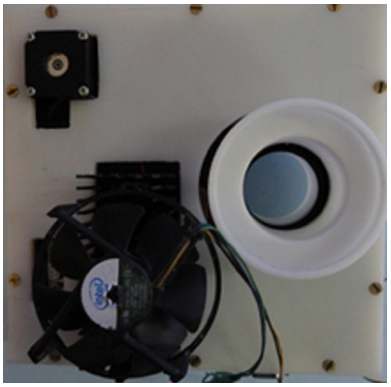

Figure 3. The outer view of the filter wheel assembly augmented with a thermal chamber after mounting all the five filters.

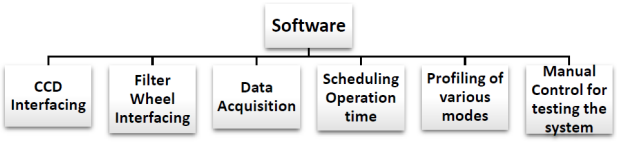

Figure 4. Various software modules necessary for making CMAP a completely automated system are shown.

3.2 Software for CMAP

CMAPs are required to be commissioned for field operations, hence, it is required that the system be fully automated. To enable automation of the system, a MFC (Microsoft Foundation Class) dialog-based software was developed in PRL. This enables operations in a programmed mode through a computer controlled software. The use of CCD as the detector for CMAP enables full automation of the system. The block diagram for the development of the software is shown in Figure 4.

3.2.1 CCD control

The CMAP software includes setting of the different CCD parameters, such as, the CCD temperature, on-chip binning, exposure time, and image acquisition. A GUI (Graphical User Interface) was developed by using the SDK (Software Development Kit) provided with the CCD. The SDK which was used for this purpose is included in the files "ArtemisHSC.h" and "ArtemisHSC.cpp", which was modified as per our requirement to automate the CCD operations.

3.2.2 Filter Wheel interface

Unlike the case for CCD, the SDK was not provided with the filter wheel (ATIK EFW2). However, the driver of the filter wheel was ASCOM compliant and that feature was made use

of as the filter wheel is accessed in the software by creating a COM object of the ASCOM compliant device. Then, using the libraries/methods of ASCOM, various functions were created so as to connect, disconnect, get position, and set position of the filter wheel. These libraries were added to the MFC based application and the functions created were called so as to interface with the filter wheel properly.

3.2.3 Data acquisition and cataloguing

For the analysis of the data it is required that all the relevant information like date, year, time, exposure time, CCD temperature, filter position, filter temperature, binning, etc., of the image being acquired be stored in a catalogue file. This is achieved by the in-house developed software. The software also creates a directory with a name of the current date and stores the images obtained with current time as the filename.

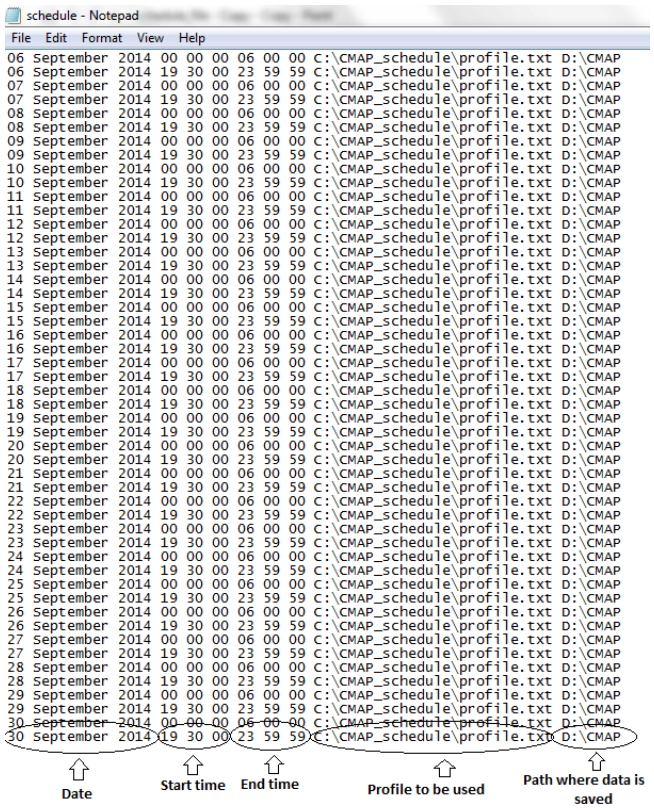

Figure 5. Sample schedule file used to operate CMAP. Different inputs as given to the in-house built software are marked out for easy understanding.

3.2.4 Profiling and scheduling

It is required to schedule the operation of all the components of CMAP and make a catalogue file which stores all the necessary parameters. This was achieved by developing appropriate codes for the different systems used in the CMAP to enable uninterrupted data acquisition. This software can accept different schedule and profile files which can be created beforehand and used for operation over long duration. The user can change the parameters as per the scientific requirement, which will be reflected in the manner in which the data acquisition is carried out by the software. With the help of this provision, the system can be operated without any human intervention.

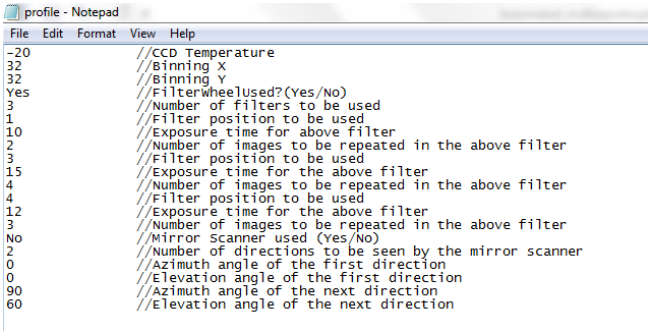

Figure 6. Sample Profile file used to input various parameters for a set of observations. The corresponding values set can also be noted on the left side.

3.2.5 Salient features of the software

To run the instrument in continuous mode the main inputs which are required to be provided are the schedule and profile files. As shown in Figure 5, the schedule file contains the start time and the end time of data acquisition by the system. It also has to be provided with the locations of the profile file and the storage of acquired data.

The profile file is the file which sets the parameters of the instrument for the duration of a single schedule. As shown in the profile format (Figure 6) it has provision for CCD binning and temperature. It has the information of all the filters to be used along with the provision for exposure times for each of them individually and number of repetitions for the filter. It also has the provision to enable mirror scanner which empowers the photometer to view in different directions. Mirror scanner is an additional attachment which can be used by the researcher as per the scientific requirement. By this arrangement, the system can acquire data for various directions with specified azimuth and elevation angles and store the information of the same. Such a dataset yields information on the spatial variations of atmospheric dynamical parameters as measured in the optical airglow emission intensities. In the absence of a mirror scanner, however, the system is programmed to operate in zenith mode, by default.

Figure 7 shows a screen-shot of the GUI of the software developed in which one can see whether filter wheel is in use, and if the status is connected[***Filter Wheel: Connected***]. The figure also shows the number of filters that are in use during the campaign along with the exposure times of each one of them and the number of images to be repeated for same filter during the observational period. If the system is to be used at a single emission wavelength it can be set in the profile that filter wheel will not be used and then it will run in single position mode continuously till the schedule ends as shown in the Figure 8.

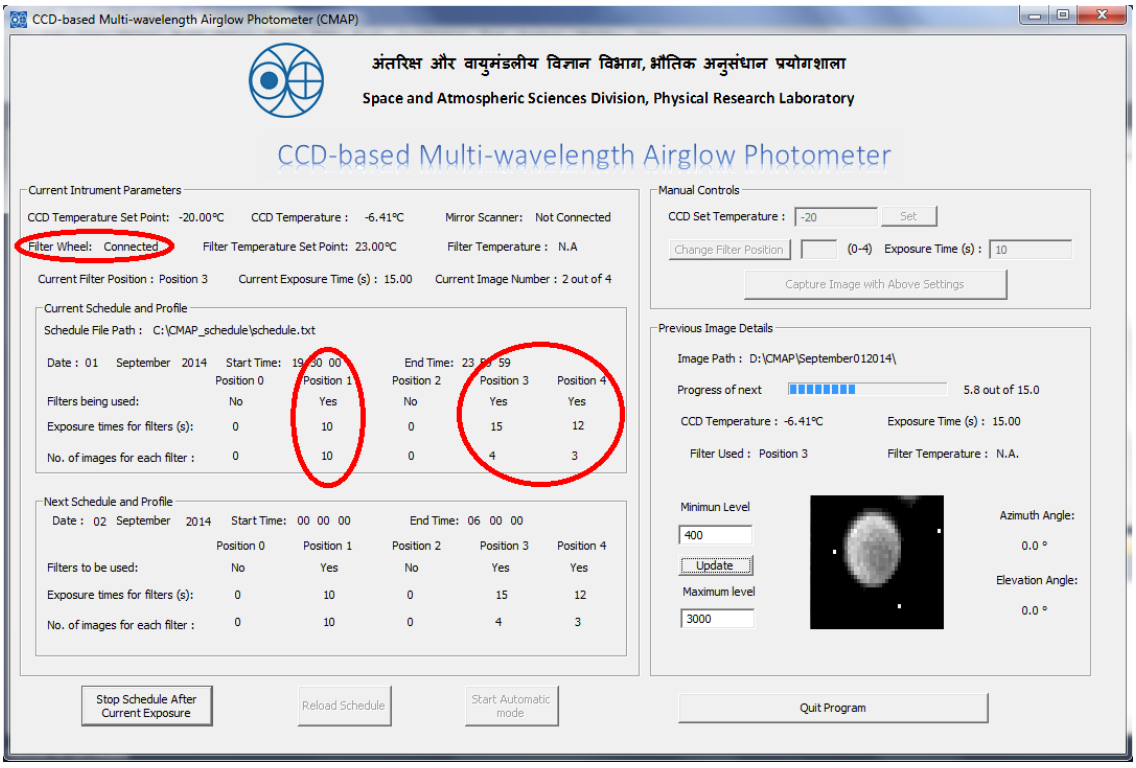

Figure 7. Screen-shot of the software while CMAP is operating. The red circles indicate that the filter wheel is connected and the positions at which CMAP is programmed to operate.

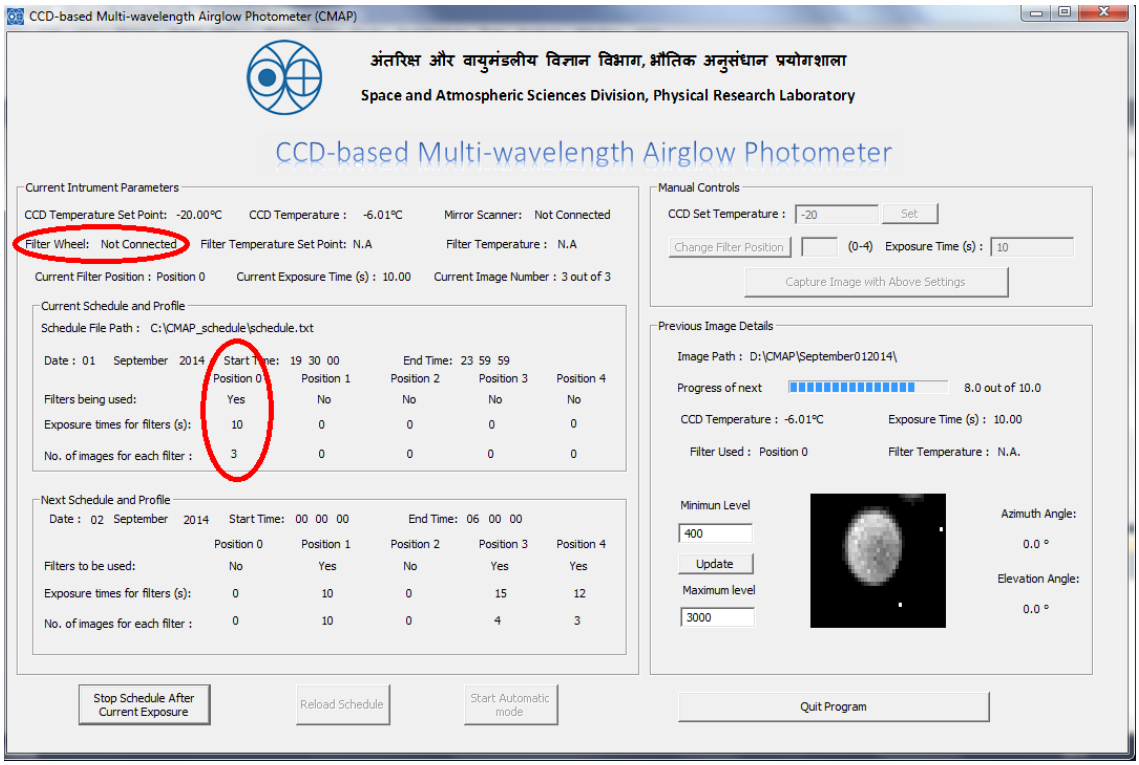

Figure 8. Screen-shot when operations are carried out for measuring emission intensities at single wavelength.

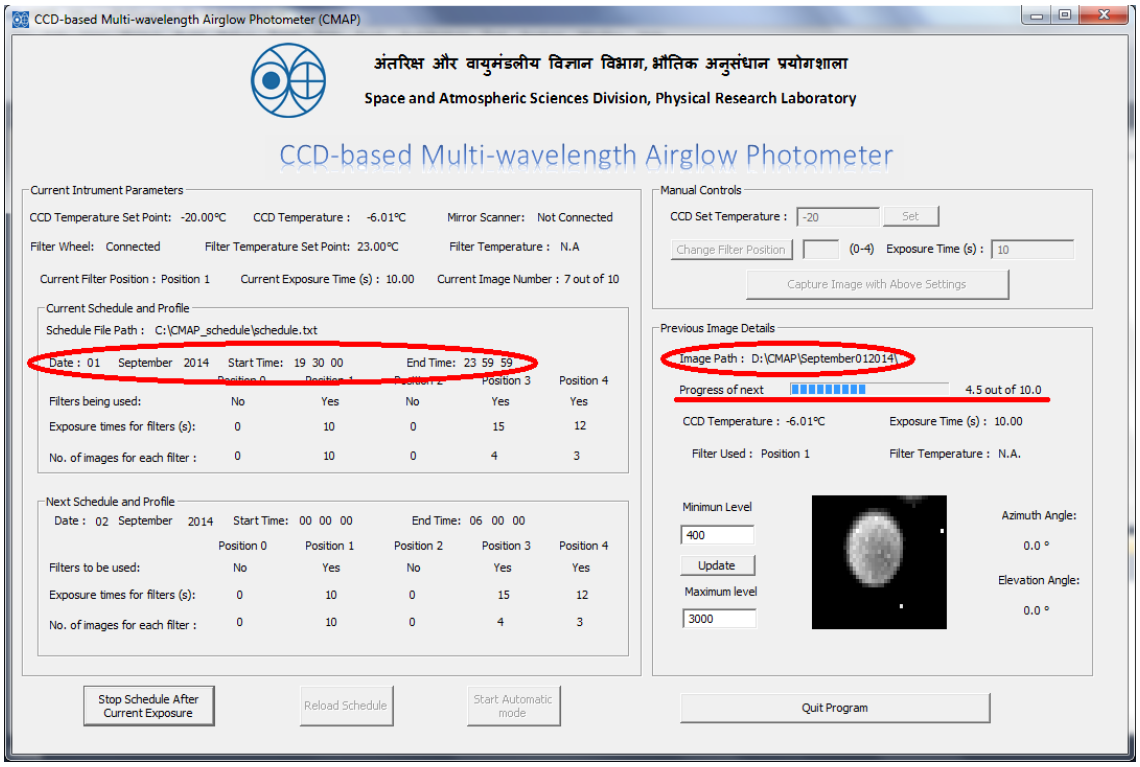

Figure 9. CMAP running in automatic mode as seen in the screen-shot of the software. Encircled parts denote the active schedule and the image save path for the current set of images obtained. Also, the underlined progress bar denotes the progress of the current exposure.

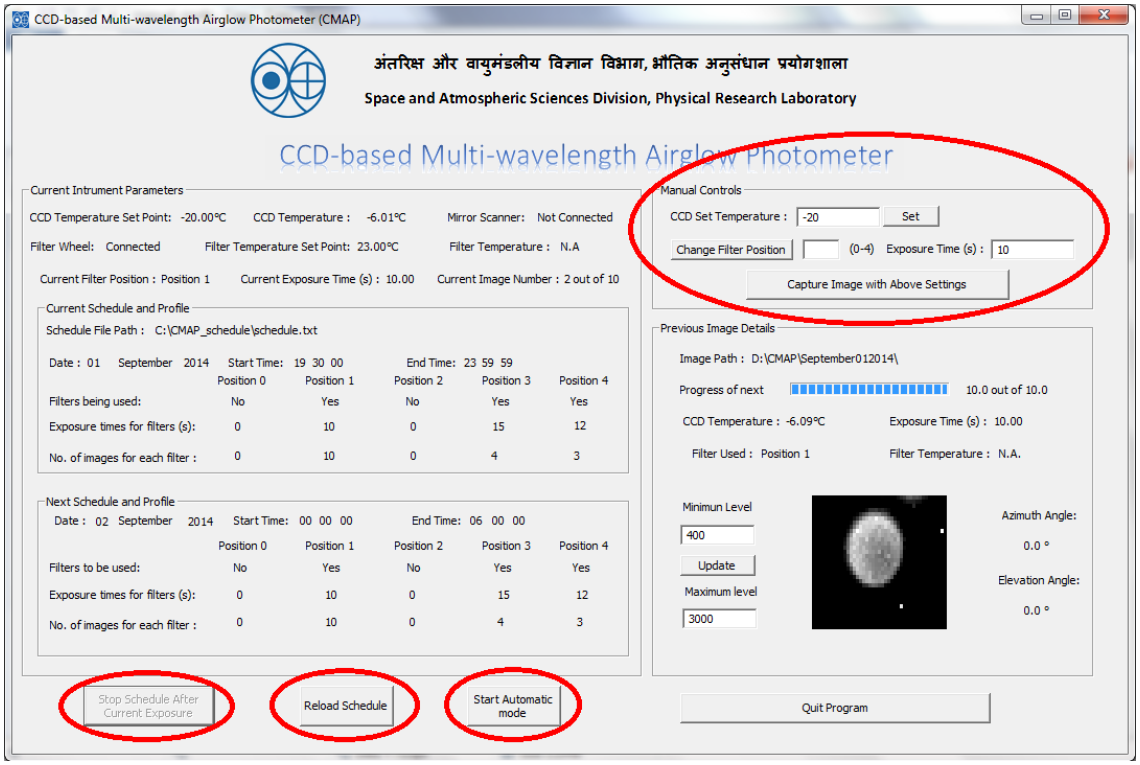

Figure 10. Screen-shot showing the manual controls such as setting CCD temperature, changing filter position, setting exposure time and taking a sample image being activated and are encircled in the figure.

Through this software the instrument will operate in an automated mode (refer Figure 9) and store the images obtained in a folder with the name as current date and year.

This software also has the provision such that the system can be operated in manual mode (refer Figure 10) which is useful to test the functioning of the system and to find out the different parameters which are needed as input to the profile file in order to schedule the system to run in fully automated mode. For this purpose, a ***Stop Schedule After Current Exposure*** button has been provided which empowers the user to manually control the system. After the completion of required tests, the schedule can be started again by clicking on the ***Start Automatic Mode*** button.

Also, the filename for each of the images is decided by the time at which the image was taken. All this information along with CCD temperature, binning, filter position, and temperature will be stored in a catalogue file (refer Figure 11) which will also be created with current date as filename.

As specified earlier, there is also provision to use a mirror scanner for observations in different directions, if required. In this case it will take a set of observations in all the viewing angles as specified in the profile file of that particular schedule.

Table 1. Characteristics of CCD-based Multi-wavelength Airglow Photometer (CMAP)

Objective lens	50 mm Diameter, 100 mm Focal Length
Aperture	9 mm Diameter
Throughput ($A\Omega$)	4 x 10^{-3} $cm^2 sr$
Collimating lens	50 mm Diameter, 100 mm Focal Length
Imaging lens	AF Nikkor f/1.8, Focal length 50mm
Optical efficiency, τ	0.23 (630.0 nm); 0.29 (557.7 nm); 0.23 (589.0 nm); 0.22 (589.6 nm)
CCD (e$^-$ photon^{-1})	Quantum efficiency, $q_{630.0nm} = 0.6$, $q_{557.7nm} = 0.64$, $q_{589.0nm} = 0.62$, $q_{589.6nm} = 0.62$; Gain, $g = 0.27 e^- DN^{-1}$
Total efficiency $Q(\lambda)$	$Q_{630.0nm} = 2.25$, $Q_{557.7nm} = 2.40$, $Q_{589.0nm} = 2.32$, $Q_{589.6nm} = 2.32$. $DN photon^{-1}$ 6.45μm 1391(H) x 1039(V) Sony ICX285AL chip
Sensitivity, S ($DNR^{-1}s^{-1}$)	50 mm Diameter, 100 mm Focal Length

4. Estimation of absolute intensities for CMAP

Nightglow emission intensities are estimated by subtracting the dark noise from the images acquired by CMAP and integrating counts in the illuminated region of the image. This

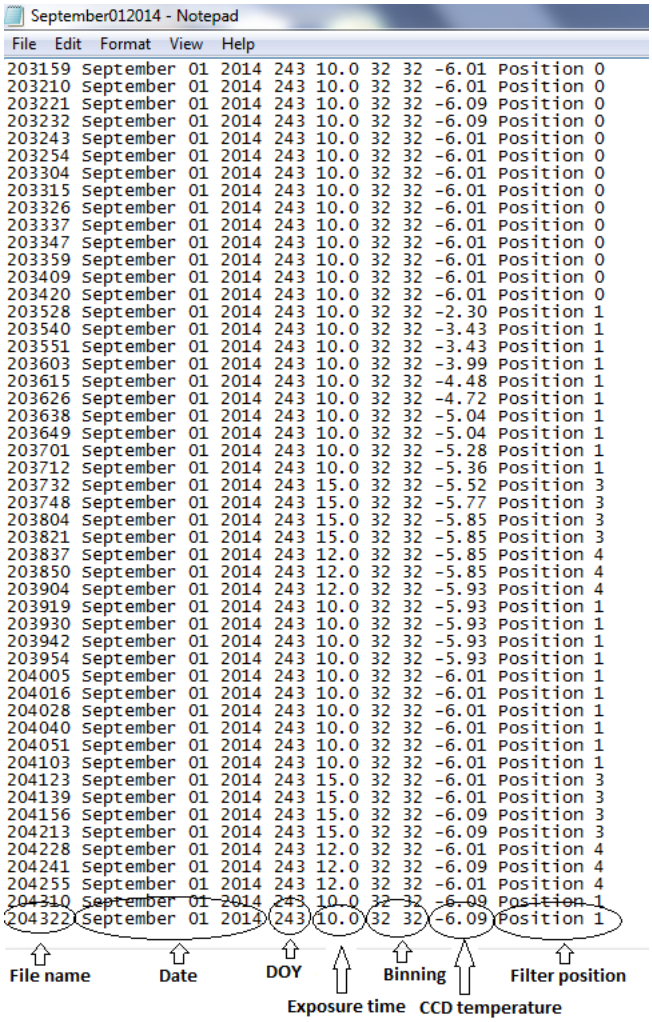

Figure 11. Sample catalogue file generated by software which maintains file name, date, day of the year, exposure time, binning, CCD temperature, filter position for all the observations.

gives an estimate of the relative intensity in data numbers (DN). One can make an approximate estimate of these intensities in Rayleighs either with a knowledge of the parameters of various components used in the instrument or by making an empirical estimate of the absolute intensities by using a lamp of known intensity at the wavelength of interest.

Here, we describe the estimation of absolute intensity with the knowledge of all the parameters of components used in building CMAP as discussed in Pallamraju et al.(2002, 2013). For a brightness B of the source in Rayleighs (R), the number of counts (N) that are registered on the CCD can be given as $N_\lambda = B_\lambda S_\lambda t$, where t is the integration time, and S is the sensitivity of the instrument expressed in DN R^{-1} s^{-1}. Sensitivity for a given wavelength for CMAP can be given as:

$$S_\lambda = \frac{10^6}{4\pi} \times \mathrm{Q}_\lambda \times \tau_\lambda \times \mathrm{A} \times \Omega \qquad (2)$$

Where, Q_λ is the overall efficiency of the CCD (quantum efficiency q_λ/ gain, g), τ_λ is the optical efficiency of the instrument, A is the area of the aperture, Ω is the solid angle of the sky that the aperture 'sees'. It is to be remembered that QE is wavelength dependent. Further, the optical efficiency comprising of transmission factors of filters and lenses used are also wavelength dependent. From the values given in Table 1 and equation 2 the sensitivity of CMAP at different wavelengths of interest has been calculated and given below:

$$S_{630.0nm} = 168.80(DNR^{-1}s^{-1}) \quad (3)$$

$$S_{557.7nm} = 224.61(DNR^{-1}s^{-1}) \quad (4)$$

$$S_{589.0nm} = 168.42(DNR^{-1}s^{-1}) \quad (5)$$

$$S_{589.6nm} = 164.07(DNR^{-1}s^{-1}) \quad (6)$$

Therefore, dividing the data numbers per second obtained by the CCD with the sensitivity values as given above for a given wavelength, one can make an estimate of the absolute emission intensities in Rayleighs. The estimated intensities in Rayleighs are shown in figures 12 and 14.

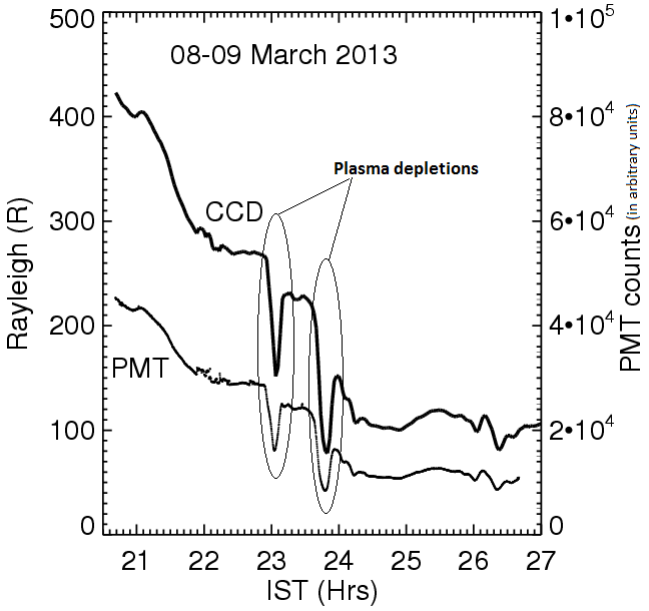

Figure 12. Inter-comparison of OI 630 nm emission between the newly built CMAP and the PMT based photometer for the night of 08 March 2013 - with plasma depletions clearly observed in both the instruments. Data are obtained from Optical Aeronomy Observatory at Gurushikhar, Mt. Abu.

5. Qualification tests for CMAP

CMAP and GUI-based software have been developed in-house, tested in the lab and commissioned at Gurushikhar, Mt. Abu for regular operations. As discussed above, the main features of this software include:

Figure 13. CMAP ready for operations.

- A single software for all the elements of the hardware (such as filter wheel, filter temperature, mirror scanner movement, all operations of CCD, etc.).
- Schedule and Profile file inputs which contain all the input parameters.
- GUI for display of all the parameters of the system.
- Provision for inclusion of attachments such as filter wheel and mirror-scanner to the system.
- Optional manual mode of operation for testing purpose.

For the purpose of comparison, CMAP was operated in simultaneity with the existing PMT-based nightglow photometer from Optical Aeronomy Observatory, Gurushikhar, Mount Abu. The results pertaining to a single wavelength (OI 630 nm) are shown in Figure 12. It is evident from the plots that CMAP shows exceptional similarity to the PMT based photometer and all the features are observed in both the photometers. Further, absolute intensities are estimated in Rayleighs for the data acquired by CMAP. It is to be noted that the initial DN obtained per second by CMAP were in the order $\sim 10^4$ and thus, Poisson statistics indicate the noise will be of the order of 100 resulting in SNR of about 100 which is very high. Hence, the error bars are not shown in the plots as they are negligible. The important aspect of the system being able to capture the events in upper atmosphere is also verified by the plots in Figure 12. Data cadence for CMAP is around sixty seconds. This is significantly smaller than the phenomenon that are of interest in aeronomy studies.

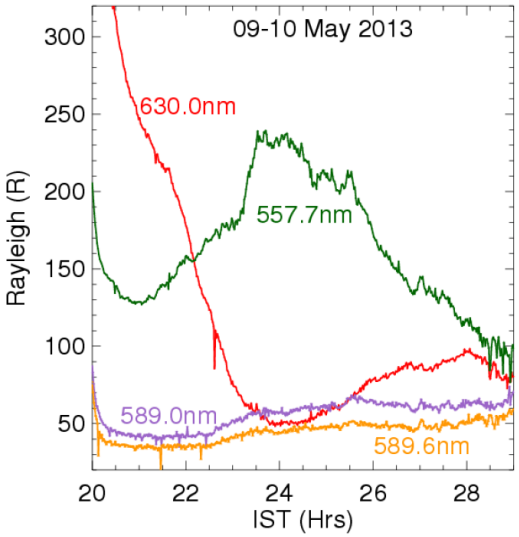

Figure 14. A sample plot of nocturnal airglow emission intensities at multiple wavelengths – Na 589.0 nm, Na 589.6 nm, OI 557.7 nm, and OI 630.0 nm from Optical Aeronomy Observatory, Gurushikhar, Mt. Abu.

For example, gravity wave periodicities are of the order of hours to several minutes, the lower cut-off being the Brunt-Vaisala period which varies from about five minutes at the lower thermospheric altitudes to around twelve minutes at the thermospheric altitudes. Thus, the data cadence of CMAP is well-suited for the investigation of nightglow emission intensities. Also, the software enables automated operation of CMAP and it can be setup in a remote field station for continuous and unattended observations. One such photometer (Figure 13) is continuously acquiring data from the Optical Aeronomy Observatory at Gurushikhar, Mt. Abu since April 2013. As we are interested in studying the dynamics at mesospheric, lower thermospheric and also at thermospheric altitudes; the airglow emissions chosen for studies are 589.0 nm, 589.6 nm, 557.7 nm, and 630.0 nm.

The sodium emissions 589.0 nm and 589.6 nm emanate from mesospheric altitudes around 88 to 97 km [Chamberlain, 1995]. Whereas, OI nightglow emission at 630.0 nm emanates from thermospheric altitudes of about 250 km and 557.7 nm emission mostly originates at around 100 km with a fraction of it coming from the thermosphere [Chamberlain, 1995]. Shown in Figure 14 is an example of one night's emission intensities as measured in near simultaneity by CMAP. As it can be seen in the absolute intensities at multiple wavelengths, on this night the maximum intensity was $\sim$ 220 R for OI 557.7 nm. The OI 630.0 nm intensity decreased from around 300 R during the twilight time to around 100 R during post-midnight hours. The Na 589.0 and 589.6 nm emission are around 50 R throughout the night. Detailed studies on the vertical coupling of atmospheres based on the CMAP data are currently underway.

6. Future plans

The successful development of both hardware and software followed by the installation of the CCD-based Multi-wavelength Airglow Photometer (CMAP) developed in-house lead to the possibility of fabrication of multiple such systems to create a network of them to study the dynamics of mesosphere, lower thermosphere, thermosphere and its coupling over spatial locations of geophysical significance. Provisions are kept for incorporating different and better CCDs as they may become available in the future. Two more such systems are being fabricated presently and are planned to be installed at different sites.

Acknowledgements

Support for fabrication of mechanical components by Shri Rajesh Kaila and other personnel of PRL's workshop is duly acknowledged. We would like to thank Mr. Sachin Panchal and Mr. Mitesh Bhavsar for their help in the development of temperature monitoring electronics. We are also thankful for the help received from certain members of ASCOM initiative group on yahoo for filter wheel interfacing. This work is supported by Dept. of Space, Govt. of India.

References

1. Chakrabarty D., PhD thesis, 2007
2. Chamberlain, Physics of the Aurora and Airglow, 1995
3. Hamamatsu, H7421 datasheet.
4. http://www.andovercorp.com/static/pdf/catalog.pdf
5. http://www.dangl.at/ausruest/atik_314/atik_314_e.htm
6. http://www.dxomark.com/Lenses/Nikon/AF-Nikkor-50mm-f-1.8D/(camera)/792
7. Pallamraju D., CAWSES-II, TG4 Newsletter Vol. 8, April, 2012
8. Pallamraju, D., CEDAR Tutorial, 2003, Errors in Airglow & Auroral Emission Measurements, http://cedarweb.hao.ucar.edu/workshop/tutorials/2003/pallamraju03.pdf.
9. Pallamraju, D., G. Lu, and C. Lin (2012), Overview of the special issue on the atmospheric coupling processes in the Sun-Earth system, J. Atmos. Sol-Terr. Phys., 75–76, 1–4
10. Pallamraju, D., J. Baumgardner, and S. Chakrabarti (2002), HIRISE: A ground-based high-resolution imaging spectrograph using echelle grating for measuring daytime airglow/auroral emissions, J. Atmos. Sol.-Terr. Phys., 64, 1581–1587, doi:10.1016/S1364-6826(02)00095-0

11. Pallamraju, D., F. I. Laskar, R. P. Singh, J. Baumgardner, and S. Chakrabarti (2013), MISE: A multiwavelength imaging spectrograph using echelle grating for daytime optical aeronomy investigations, J. Atmos. Sol.-Terr. Phys., doi:10.1016/j.jastp.2012.12.003

12. Priedhorsky, W. C., Contrast and signal-to-noise ratio in long-distance starlight imaging, Appl. Opt., 35, 21, 4173, 1996

13. Sekar, R., Chakrabarty, D., Pallamraju, D., 2012. Optical signature of shear in the zonal plasma flow along with a tilted structure associated with equatorial spread F during a space weather event. Journal of Atmospheric and Solar- Terrestrial Physics 75-76, 57–63.

14. Thorne, A., U. Litzen, S. Johansson; Spectrophysics: Principles and Applications, Springer-Verlag Berlin Heidelberg, 1999.

PRL research encompasses the earth the sun immersed in the fields and radiations reaching from and to infinity, all that man's curiosity and intellect can reveal

पीआरएल के अनुसंधान क्षेत्र में समविष्ट हैं पृथ्वी एवं सूर्य जो निमीलित हैं चुंबकीय क्षेत्र एवं विकिरण में अनंत से अनंत तक जिन्हे प्रकट कर सकती है मानव की जिज्ञासा एवं विचारशक्ति